

# Superradiant Quantum Phase Transition in Open Systems: System-Bath Interaction at the Critical Point

Daniele Lamberto,<sup>1</sup> Gabriele Orlando,<sup>1</sup> and Salvatore Savasta<sup>1</sup>

<sup>1</sup>*Dipartimento di Scienze Matematiche e Informatiche,  
Scienze Fisiche e Scienze della Terra, Università di Messina, I-98166 Messina, Italy*

The occurrence of a second-order quantum phase transition in the Dicke model is a well-established feature. On the contrary, a comprehensive understanding of the corresponding open system, particularly in the proximity of the critical point, remains elusive. When approaching the critical point, the system inevitably enters first the system-bath ultrastrong coupling regime and finally the deep strong coupling regime, causing the failure of usual approximations adopted to describe open quantum systems. We study the interaction of the Dicke model with bosonic bath fields in the absence of additional approximations, which usually relies on the weakness of the system-bath coupling. We find that the critical point is not affected by the interaction with the environment. Moreover, the interaction with the environment is not able to affect the system ground-state condensates in the superradiant phase, whereas the bath fields are *infected* by the system and acquire macroscopic occupations. The obtained reflection spectra display lineshapes which become increasingly asymmetric, both in the normal and superradiant phases, when approaching the critical point.

## I. INTRODUCTION

The Dicke model was one of the first models historically introduced in the study of the light-matter interaction [1–3]. It was firstly utilized to describe the interaction of a single cavity mode with a collection of  $N$  atomic dipoles, treated as two-level systems (TLSs). This model exhibit a second-order equilibrium phase transition when the coupling strength exceeds a critical value, entering a phase in which the collective atomic polarization and the photonic field are finite even at zero temperature and without external driving. This widely studied phenomenon [4, 5] is known as superradiant phase transition (SPT), and is also referred as ground-state photon condensation [6, 7]. The Dicke model Hamiltonian also exhibits a quantum phase transition (QPT) [8], which can occur at zero temperature [9–11] by tuning the light-matter coupling across a quantum critical point. However, according to a number of no-go theorems SPT (and also the corresponding QPT [9, 12, 13]) is forbidden for systems interacting with photons by only their electric polarization [6, 9, 12, 14]. Technically, in the Coulomb gauge, it is the diamagnetic term in the Hamiltonian, neglected in the Dicke model, which prevents the SPT [12, 15].

This equilibrium SPT has been attracting enduring attention since several decades, but its experimental demonstration still remains very challenging, despite numerous proposals put forward over the years to realize systems mimicking an effective Dicke Hamiltonian [16]. Non-equilibrium realizations of SPTs have been reported, e.g., in cold-atom systems driven by laser fields [17–22] and trapped ions [23]. However, despite strong analogies with the equilibrium SPT, non-equilibrium SPTs in driven-dissipative system are inherently different phenomena [4, 24–27].

Theoretical proposals for the observation of equilibrium SPTs consider circuit QED systems [9, 28–32], elec-

tron gases that either display a Rashba spin-orbit coupling [33] or interact with a spatially varying electromagnetic field [33–35], magnetic molecules that couple to superconducting microwave resonators via the Zeeman interaction [7, 36, 37]. A recent proposal [38] considering  $\text{Er}^{3+}$  spins cooperatively interacting with a magnonic field playing the role of photons, has led to the first (at our knowledge) spectroscopic evidence for an equilibrium SPT [39].

The SPT has been exhaustively studied theoretically in the isolated system, both at zero temperature and not [2, 10, 11]. It has been shown that the system ground state display a quantum squeezed vacuum on a photon-atom two-mode basis which reaches perfect squeezing at the SPT critical point. Moreover, the ground-state entanglement between the atoms and the field diverges logarithmically at the critical coupling for  $N \rightarrow \infty$  [40].

On the other hand, no clear understanding for the open system counterpart has been reached yet in the proximity of the QPT critical point, especially when considering the equilibrium SPT. Given the recent progress [39], which reported the first long-sought experimental observation of an equilibrium SPT at low temperatures, a fully and rigorous quantum treatment of the open Dicke model is required. Moreover, an accurate description of decoherence and of the relationship between the system and the input-output fields near critical points is essential for the development of criticality-enhanced quantum sensing [41, 42].

A key feature of the equilibrium SPT in the thermodynamic limit is the softening of the lowest polariton mode, which vanishes at the critical point, signaling that the transition to a photon condensate state is a second-order quantum phase transition. This implies that the usual approximations employed when studying open quantum systems, based on the smallness of the ratio between the loss rate and the relevant resonance frequencies of the system  $\gamma/\omega$  fail. At a certain point, sufficiently close to the critical point, the system inevitably

enters first the system-bath ultrastrong coupling regime [43, 44] ( $\gamma/\omega > 0.1$ ) and finally the deep strong coupling regime ( $\gamma/\omega > 1$ ).

A number of questions remain open: (i) What is the impact of these system-bath extreme interaction regimes on the QPT? (ii) Assuming that the environment does not destroy the QPT, how it affects the critical point and the ground state condensates? (iii) Are the external thermal baths affected by the QPT? (iv) Can the properties of the system ground state be observed via an input-output port? (v) How to calculate the (observed [39]) spectroscopic features in proximity of the critical point? (vi) How the answers to the above results depend on the specific spectral densities of the thermal baths?

In this paper we present a full quantum description of the open Dicke model, based on the quantum Langevin equations, which is not restricted by the smallness of  $\gamma/\omega$  and that can be applied for essentially any range of parameters, differently from those approaches (as the Limblad master equation) which rely on the rotating wave approximation (RWA) or the weakness of the system-bath interaction. The framework presented here is able to accurately describe the equilibrium open Dicke model in the proximity of the mode softening. In particular, the critical point of the open Dicke model can be identified in a fully quantum framework and without relying on the mean field theory. Within this approach, the superradiant phase of the open Dicke model is faced by diagonalizing the full Hamiltonian describing the open quantum system. We find that a large class of thermal baths consisting of an infinite number of harmonic oscillators (normal modes) interacting with the system via a potential displaying a metastable minimum and with a *well-behaved* density of states (properly vanishing as  $\omega \rightarrow 0$ ) do not affect the critical point of the corresponding closed system. This result is in agreement with recent experimental results [39] and in contrast with previous theoretical findings for driven-dissipative systems based on the master equation approach [45–47]. We will also show that the ground state condensation occurring in the system influences the bath state, but not vice-versa. This theoretical framework allows us to calculate the spectral properties of the system when probed by a coherent weak tone at any value of the critical parameters, for different baths spectral densities and for arbitrary large damping rates.

## II. STANDARD DICKE MODEL AND SUPERRADIANT PHASE TRANSITION

In this section, we briefly present the main features of the Dicke model for an isolated system, i.e. without considering its interaction with the external environment. The Dicke Hamiltonian, which describes a single bosonic mode with frequency  $\omega_a$  interacting with a collection of  $N$  identical TLSs with transition frequency  $\omega_b$ , can be

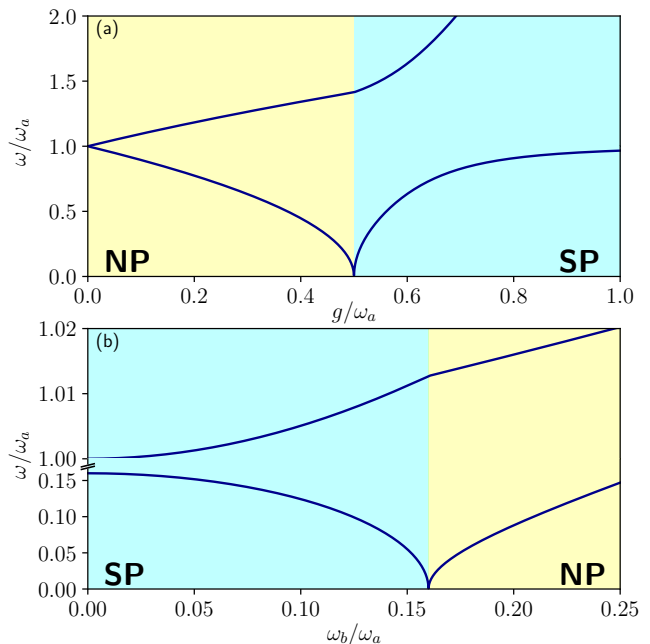


FIG. 1. **Excitation energies of the isolated system.** Upper and lower excitation energies for the isolated system in the normal (yellow background) and superradiant (cyan background) phases as a function of the (a) normalized coupling and (b) frequency ratio. Parameters: (a)  $\omega_0/\omega_c = 1$ , (b)  $g/\omega_c = 0.2$ .

written as

$$H = \hbar\omega_a a^\dagger a + \hbar\frac{\omega_b}{2} \sum_{i=1}^N \sigma_i^z + \hbar\frac{g}{\sqrt{N}} (a^\dagger + a) \sum_{i=1}^N \sigma_i^x, \quad (1)$$

where  $a$  is the bosonic operator,  $\sigma_i^\alpha$  (with  $\alpha = x, y, z$ ) are the usual Pauli operators associated to the  $i$ -th TLS and  $g$  is the coupling constant (for simplicity, we considered that all the TLSs couple with the bosonic mode with the same intensity). Eq. (1) can be simplified by the introduction of collective atomic operators  $J^\alpha = \sum_i \sigma_i^\alpha$ , satisfying the usual angular momentum algebra. We focus our study on the manifold of maximum angular momentum, which is composed by states that maximally couple with the bosonic field. This corresponds to fixing  $j = N/2$ , with  $j$  being the eigenvalue of the total angular momentum operator  $\mathbf{J}^2$ . We now introduce the Holstein-Primakoff (HP) transformations defined by [48–50]  $J^z = \hbar(b^\dagger b - \frac{1}{2})$ ,  $J^+ = \hbar b^\dagger \sqrt{N - b^\dagger b}$  and  $J^- = (J^+)^\dagger$ , which yields to the bosonic version of the Dicke Hamiltonian

$$H = \hbar\omega_a a^\dagger a + \hbar\omega_b b^\dagger b + \hbar g (a^\dagger + a) \left( b^\dagger \sqrt{1 - \frac{b^\dagger b}{N}} + \sqrt{1 - \frac{b^\dagger b}{N}} b \right). \quad (2)$$

As it is well-known, in the thermodynamic limit (corresponding to  $N \rightarrow \infty$ , while  $\rho = N/V$  remains finite),

such Hamiltonian predicts a QPT for a critical coupling  $g_c = \sqrt{\omega_a \omega_b}/2$  [9, 10]. For  $g > g_c$  the fields acquire macroscopic ground state occupations, thus structurally changing the properties of the system. On the contrary, in the so-called *normal phase* ( $g < g_c$ ), the ground state of the system does not exhibit any condensation and thus, in the low-excitation regime, the lowering and raising operators in the HP maps can be linearized, leading to effective Hamiltonian for the normal phase

$$H_{\text{NP}} = \hbar\omega_a a^\dagger a + \hbar\omega_b b^\dagger b + \hbar g (a^\dagger + a) (b^\dagger + b). \quad (3)$$

Such Hamiltonian can be diagonalized by considering the Hopfield-Bogoliubov matrix  $\mathbf{A}$ , whose eigenvalues represent the excitation energies of the system. The matrix  $\mathbf{A}$ , in the normal phase, is given by

$$\mathbf{A}_{\text{NP}} = \begin{pmatrix} \omega_a & 0 & g & g \\ 0 & -\omega_a & -g & -g \\ g & g & \omega_b & 0 \\ -g & -g & 0 & -\omega_b \end{pmatrix} \quad (4)$$

As expected, the lower excitation energy  $\omega_-$  vanishes as  $g \rightarrow g_c$ , thus signaling the presence of a QPT. In contrast, in the *superradiant phase* obtained for  $g > g_c$ , both fields acquire a macroscopic coherent occupation. To take into account the condensation, we shift the bosonic operators as  $a = a_s + \sqrt{\alpha}$  and  $b = b_s - \sqrt{\beta}$ , where  $\alpha$  and  $\beta$  are c-number of order  $O(N)$ , while  $a_s$  and  $b_s$  are still bosonic operators describing the fluctuations with respect to the respective mean value. Inserting these definitions into Eq. (2) and imposing an equilibrium condition in the resulting expression (corresponding to the vanishing of the linear terms in these bosonic operators), we obtain non-zero macroscopic mode occupations in the superradiant phase, given by

$$\alpha = \frac{Ng^2}{\omega_a^2} \left(1 - \frac{1}{\lambda^2}\right), \quad \beta = \frac{N}{2} \left(1 - \frac{1}{\lambda}\right) \quad (5)$$

where  $\lambda = 4g^2/\omega_a\omega_b = g^2/g_c^2$ . Hence, the Hamiltonian in the superradiant phase is

$$H_{\text{SP}} = \omega_a a_s^\dagger a_s + \tilde{\omega}_b b_s^\dagger b_s + \tilde{g} (a_s + a_s^\dagger) (b_s + b_s^\dagger) + D (b_s + b_s^\dagger)^2 \quad (6)$$

where  $\tilde{\omega}_b = \omega_b(\lambda + 1)/2$ ,  $\tilde{g} = g_c \sqrt{2/(\lambda + 1)}$  and  $D = \omega_b(\lambda - 1)(3\lambda + 1)/8(\lambda + 1)$ . The Hopfield-Bogoliubov matrix in the superradiant phase is

$$\mathbf{A}_{\text{SP}} = \begin{pmatrix} \omega_a & 0 & \tilde{g} & \tilde{g} \\ 0 & -\omega_a & -\tilde{g} & -\tilde{g} \\ \tilde{g} & \tilde{g} & \tilde{\omega}_b + 2D & 2D \\ -\tilde{g} & -\tilde{g} & -2D & -\tilde{\omega}_b - 2D \end{pmatrix} \quad (7)$$

In Fig. 1 are plotted the upper and lower excitation energies of the standard (closed system) Dicke model as a function of the normalized coupling strength  $g/\omega_a$  Fig. 1(a) and of the ratio between the frequencies  $\omega_b/\omega_a$  Fig. 1(b).

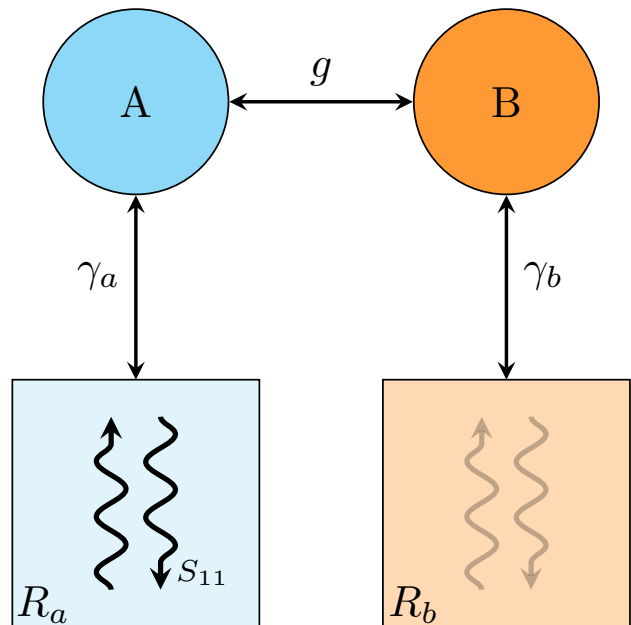


FIG. 2. **Sketch of the generic system investigated here.** Two interacting subsystems, A and B, with coupling constant  $g$ . Each component interacts with its own thermal bath. The interaction of a subsystem with its own reservoir can also be regarded as an input-output port, through which the system can be excited and probed. In this work we will consider explicitly a single tone coherent excitation of subsystem A and we calculate the corresponding reflection coefficient  $S_{11}$ . This framework can be easily generalized to include the interaction with additional thermal baths.

### III. OPEN DICKE MODEL

In this section, we extend the study of the well-established Dicke model and of its superradiant quantum phase transition, to include its interaction with the external environment. While many approaches have been developed during the years for the study of the driven-dissipative Dicke model, the lack of a general theory able to describe a non-driven QPT in presence of losses, not relying on those approximations which fail in proximity of the critical point (e.g. Born-Markov and rotating wave approximations), is still missing, at least to our knowledge. We present here a general theoretical framework based on the Quantum Langevin equations, valid both in the normal and superradiant phase, which is approximation-free, thus suitable for the description of the non-driven dissipative QPT. Furthermore, this approach enables the calculation of reflection, absorption, and transmission spectra for arbitrary values of the coupling strength and loss rates. In our derivation, we consider the general case in which both the subsystems interact with their respective external environments through the decay rates  $\gamma_a$  and  $\gamma_b$ , respectively (see Fig. 2). This treatment can be easily extended in the case of additional losses, such as additional input-output ports or

non-radiative losses, which have not been included for the sake of simplicity. As usual, the external baths are taken as infinite, discrete collections of independent harmonic oscillators, coupled to the system Hamiltonian through their coordinates [51]. Hence, the total Hamiltonian is given by

$$H_{\text{tot}} = H_{\text{sys}} + \frac{1}{2} \sum_{j=a,b} \sum_n [p_{jn}^2 + k_{jn}(q_{jn} - X_j)^2], \quad (8)$$

where  $q_{jn}$  and  $p_{jn}$  are the coordinate and the momentum related to the  $n$ -th mode of the  $j$ -th oscillator, respectively, and  $X_j$  are the systems coordinates. This coupling is physically well-grounded, as it makes the system-bath potential energy depend on the deviation of the system coordinates  $X_j$  from the corresponding bath coordinates  $q_{jn}$ . Moreover, this interaction potential displays a metastable energy minimum. Another commonly used form of the system-bath interaction term is typically expressed as a sum of products between the coordinates,  $q_{jn}X_j$ . Differently from the form in Eq. (8), the latter does not display an energy minimum and can thus introduce additional instabilities in the system description. As we will see, the form of the interaction potential can have relevant consequences on the SPT of the open Dicke model. Throughout this paper, we base our analysis on the system described by Hamiltonian in Eq. (8) and investigate the open system dynamics using quantum Langevin equations, without introducing any additional approximation to the system-bath interaction. An equivalent alternative approach involves the Fano-Hopfield-Bogoliubov diagonalization of the full Hamiltonian (see, e.g., Refs [52, 53]).

### A. Normal Phase

By performing a canonical transformation to simplify the calculations, Eq. (8) can be rewritten in the form

$$H = H_{\text{sys}} + \frac{1}{2} \sum_{j=a,b} \sum_n [(p_{jn} - \sqrt{k_{jn}}X_j)^2 + \omega_{jn}^2 q_{jn}^2], \quad (9)$$

where the coupling now involves the bath momenta  $p_{jn}$ . The systems  $A$  and  $B$  coordinates in Hamiltonian (9) are  $X_a = a^\dagger + a$  and  $X_b = b^\dagger \sqrt{1 - b^\dagger b/N} + \sqrt{1 - b^\dagger b/N} b$ , respectively. In the thermodynamic limit, the ground state in the normal phase is not macroscopically occupied, hence, the square root in the definition of the system  $B$  coordinate can be approximated to unity, leading to the effective coordinate  $X_b = b^\dagger + b$ . From Eq. (9), we can effectively trace out the bath degrees of freedom and derive the corresponding quantum Langevin equations which, in the Fourier domain, are [51]

$$-i\omega \mathbf{v}(\omega) = -i \left( \mathbf{A} - \frac{i}{2} \mathbf{\Gamma}(\omega) \right) \mathbf{v}(\omega) + \tilde{\mathbf{F}}_{\text{in}}(\omega) \quad (10)$$

where  $\mathbf{v} = (\tilde{a}, \tilde{a}^\dagger, \tilde{b}, \tilde{b}^\dagger)^T$  and  $\tilde{\mathbf{F}}_{\text{in}}$  is the Langevin forces vector in the frequency domain (see App. A). The decay matrix  $\mathbf{\Gamma}$  depends on how the losses of the system are modeled, which in turn are linked to the bath-system couplings  $k_{jn}$ . To simplify the notation, from now on we will omit the explicit dependence on  $\omega$  whenever it is not strictly necessary. By introducing the matrix  $\mathbf{M}(\mathbf{A}, \mathbf{\Gamma}) = \mathbf{A} - i\mathbf{\Gamma}/2 - \omega \mathbf{I}$ , Eq. (10) can be written compactly as

$$\tilde{\mathbf{F}}_{\text{in}} = i\mathbf{M}(\mathbf{A}, \mathbf{\Gamma}) \mathbf{v} \quad (11)$$

For the specific cases of only one bath for each of the two components (see Fig. 2), the resulting decay matrix  $\mathbf{\Gamma}$  can be expressed in the normal phase as

$$\mathbf{\Gamma}_{\text{NP}} = \begin{pmatrix} \gamma_a & -\gamma_a & 0 & 0 \\ -\gamma_a & \gamma_a & 0 & 0 \\ 0 & 0 & \gamma_b & -\gamma_b \\ 0 & 0 & -\gamma_b & \gamma_b \end{pmatrix}, \quad (12)$$

If the system is not coherently driven, the mean values of the input fields vanish. Hence, by taking the average of Eq. (11), we obtain the complex eigenvalues of the equilibrium open Dicke model by imposing the compatibility constraint on the system of equations (11), given by the solutions of the equation

$$\zeta(\omega; \omega_a, \omega_b, \gamma_a, \gamma_b) \equiv \det[\mathbf{M}(\omega; \mathbf{A}, \mathbf{\Gamma})] = 0. \quad (13)$$

Eq. (13) is to be specialized in the normal phase upon the use of the corresponding  $\mathbf{A}_{\text{NP}}$  and  $\mathbf{\Gamma}_{\text{NP}}$ , i.e.  $\zeta_{\text{NP}}(\omega) = \det[\mathbf{M}(\omega; \mathbf{A}_{\text{NP}}, \mathbf{\Gamma}_{\text{NP}})]$ . The behavior of  $\zeta_{\text{NP}}(\omega)$  (hence, in the normal phase) is plotted in Fig. 3 on the yellow background, as it will be discussed in greater details in Sec. III C. Here, we restrict our discussion to noticing that the critical point of the open system can be identified as the same of the corresponding isolated Dicke model. Beyond this critical point, the ground state of the system acquires a macroscopic occupation, imposing a modification in our description of the system. In the following section, we will explore this adaptation in detail.

### B. Superradiant Phase

To accurately describe the properties of the open Dicke model in the superradiant phase, it is essential to account for the condensation that occurs in the ground state of the system. To this end, as in the standard Dicke model for an isolated system, we shift the bosonic operators describing our system as

$$\begin{cases} a = a_s + \sqrt{\alpha} \\ b = b_s - \sqrt{\beta} \\ c_m = c_{s,m} + i\sqrt{\tau_m} \\ d_n = d_{s,n} - i\sqrt{\sigma_n} \end{cases} \quad (14)$$

where as usual we introduced bosonic operators,  $c_m = (\omega_{am} q_{am} + i p_{am}) / \sqrt{2\hbar\omega_{am}}$  and

$d_n = (\omega_{bn}q_{bn} + ip_{bn})/\sqrt{2\hbar\omega_{bn}}$  for bath  $A$  and  $B$ , respectively. The operators with the subscript  $s$  refer to shifted operators, representing fluctuations with respect to the corresponding mean values. By introducing such shifts into Eq. (9) and minimizing the resulting Hamiltonian, equivalent to the vanishing of the linear terms, we obtain the non-zero macroscopic occupations (see App. B)

$$\begin{cases} \alpha = \frac{Ng^2}{\omega_a^2} \left(1 - \frac{1}{\lambda^2}\right) \\ \beta = \frac{N}{2} \left(1 - \frac{1}{\lambda}\right) \\ \tau_m = 2 \frac{k_{am}}{\omega_{am}} \alpha \\ \sigma_n = 2 \frac{k_{bn}}{\omega_{bn}} \beta \end{cases} \quad (15)$$

where  $\lambda = 4g^2/(\omega_a\omega_b)$ . Remarkably, this minimization procedure, outlined in App. B, reveals that the open Dicke model predicts a macroscopic ground state condensation in the superradiant phase which is exactly the same as in the isolated system, as testified by the same values of  $\alpha$  and  $\beta$  as in the Sec. II. These results highlight what we could define a resilience of the condensate to the system opening. Moreover, such ground state condensation of the systems (even if not influenced by the presence of the baths as already stressed) induces nonetheless a macroscopic occupation in the bath fields. This phenomenon is to be expected in an equilibrium situation since it can be interpreted as the baths being infected by the system property, e.g. analogously to a magnetization induced in a material brought into contact with a magnet. We identify two primary motivations underlying these results: first, the equilibrium state between the system and the bath, and second, the specific form of the system-bath coupling as defined in Eq. (8). Regarding the latter, we emphasize that the choice of the coupling is physically well-grounded given its straightforward physical interpretation, i.e. the coordinates of the baths  $q_{jn}$  get shifted by the system coordinates  $X_j$ . Another commonly adopted approach involves considering an interaction term that includes only the product of the coordinates  $q_{jn}X_j$ , excluding the quadratic term  $X_j^2$ . The main advantage of opting for a potential of the former type, rather of the latter, lies in its defined positive nature. This ensures the presence of an energy minimum, thereby avoiding the introduction of additional instabilities into the system. It should now be evident that the choice of microscopic interaction significantly influences the resulting outcomes. For instance, the compensation among terms during the minimization process to determine the macroscopic mode occupations (see App. B) is directly tied to this choice. Consequently, alternative choices could yield different predictions.

The resulting effective Hamiltonian in the superradiant phase is given by

$$H = H_{\text{SP}} + \frac{1}{2} \sum_{j=a,b} \sum_n \left[ \left( \rho_{jn} - \sqrt{\tilde{k}_{jn}} x_j \right)^2 + \omega_{jn}^2 q_{jn}^2 \right] \quad (16)$$

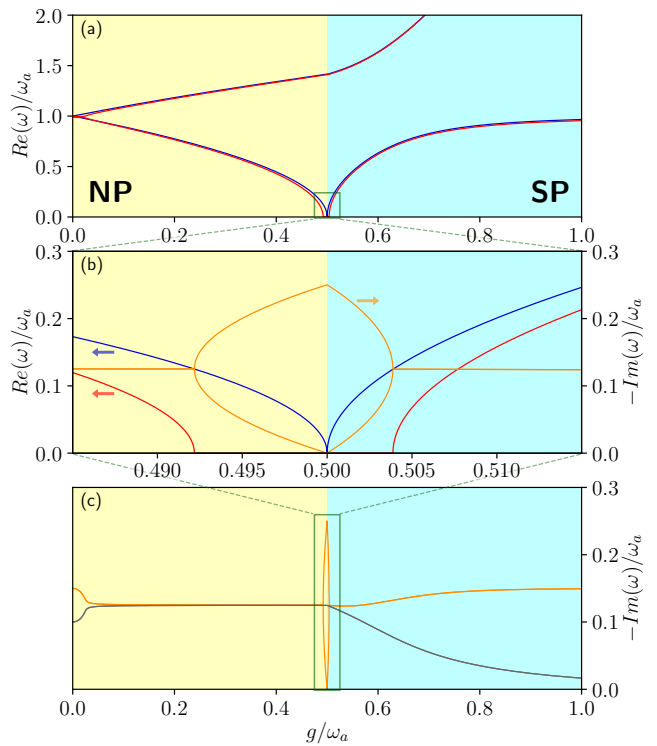


FIG. 3. **Excitation energies.** (a) Upper and lower excitation energies as a function of the normalized coupling in the closed (blue) and open (red, real parts) Dicke models. (b) Inset near the critical point of the lower polaritons of both the closed and open Dicke models. (c) Negative imaginary parts of the upper (grey) and lower (yellow) excitation energies. Parameters used:  $\omega_a = \omega_b = 1$ ,  $\gamma_a = 0.3$ ,  $\gamma_b = 0.2$ .

where we have defined the momentum fluctuations  $\rho_{am} = i\sqrt{\omega_{am}}/2(c_{s,m}^\dagger - c_{s,m})$  and  $\rho_{bn} = i\sqrt{\omega_{bn}}/2(d_{s,n}^\dagger - d_{s,n})$ , while  $x_a = a_s^\dagger + a_s$  and  $x_b = b_s^\dagger + b_s$  are the effective operators that couple with the baths. The coupling constant of system  $B$  is renormalized as  $\tilde{k}_{bn} = 4k_{bn}/(\lambda+1)^2$ , while  $\tilde{k}_{an} = k_{an}$  remains unchanged. As shown in App. B, the quantum Langevin equations in the superradiant phase preserve the same structure as in Eq. (11), upon the introduction of the decay matrix  $\mathbf{\Gamma}_{\text{SP}}$ , obtained by replacing  $\gamma_b$  with  $\tilde{\gamma}_b$ , where  $\tilde{\gamma}_b = 4\gamma_b/(\lambda+1)^2$ . Analogously, we can calculate the excitation energies in the superradiant phase by using Eq. (13), obtaining  $\zeta_{\text{SP}}(\omega) = \det[\mathbf{M}(\omega; \mathbf{A}_{\text{SP}}, \mathbf{\Gamma}_{\text{SP}})]$ . In Fig. 3 are plotted the zeros of  $\zeta_{\text{SP}}(\omega)$  on the cyan background.

### C. Excitation Energies

In Fig. 3 we plot the real (red line) and imaginary parts (yellow and grey lines, corresponding to the lower and upper polaritons, respectively) of the complex excitation energies obtained through the use of Eq. (13). The main difference between the excitation energies of the closed and open systems is the presence of a *gap* re-

gion (Fig. 3b), where the real part of the lower polariton becomes zero while the respective imaginary part splits. We identify the critical point of the QPT with the vanishing of the imaginary part of a complex excitation energy, since causality implies that response functions have no poles in the upper half complex plane. Indeed, it is worth noting that extending the normal-phase excitation frequencies beyond the critical point would predict a negative imaginary component for the lower excitation energy, thereby violating the principle of causality. We will see in the next section that the poles of a causal response function in the frequency domain (the reflection coefficient  $S_{11}$ ) actually correspond to the solutions of Eq. (13). We notice that the critical point of the QPT corresponds to the vanishing of the complex excitation energies, both in real and imaginary part.

Remarkably, it can be shown analytically that the critical point in this equilibrium open Dicke model coincides with the critical point of the corresponding standard model,  $g_c$ , given that the dissipation rates are *well-behaved*, even if not ohmic. To this end, we analyze the behavior of the complex excitation energies in the normal phase using equation Eq. (13). Within the normal phase, this yields an explicit expression given by

$$\zeta_{\text{NP}}(\omega) = \omega^4 + i(\gamma_a + \gamma_b)\omega^3 - (\omega_a^2 + \omega_b^2 + \gamma_a\gamma_b)\omega^2 - i(\omega_a^2\gamma_b + \omega_b^2\gamma_a)\omega - 4g^2\omega_a\omega_b + \omega_a^2\omega_b^2. \quad (17)$$

As can be readily observed, in the limit  $\omega \rightarrow 0$  (i.e., near the quantum phase transition), only the constant terms in Eq. (17) remain significant. These terms vanish for the same value of the coupling constant,  $g = \sqrt{\omega_a\omega_b}/2 = g_c$ , which defines the critical coupling at which the SPT occurs in the standard Dicke model. This demonstrates that the critical coupling for the SPT in the open and closed Dicke model are identical. Eq. (17) remains valid for any physically meaningful damping rates, including those that are not strictly ohmic. By this, we refer to the condition that  $\omega\gamma(\omega)$  must vanish as  $\omega \rightarrow 0$ , though the rate at which it approaches zero may vary [54]. The case of constant decay rates  $\gamma_j(\omega) \equiv \gamma_{0j}$  (for frequencies  $\omega$  much less than a characteristic cutoff frequency) corresponds to *ohmic* dissipation of Ref. [54], and gives rise to the usual velocity-dependent dissipative term of the classical damped harmonic oscillator. For example, for oscillator  $A$  we obtain the following equation of motion ( $g = 0$ ) in the frequency domain

$$-i\omega\tilde{p}_a = -\omega_a^2\tilde{q}_a - i\omega\gamma_a\tilde{q}_a + \tilde{\xi}_a, \quad (18)$$

where  $\tilde{q}_a = \sqrt{\hbar/2\omega_a}(\tilde{a}^\dagger + \tilde{a})$  and  $\tilde{p}_a = i\sqrt{\hbar\omega_a/2}(\tilde{a}^\dagger - \tilde{a})$ . Considering the condition that  $\gamma_j^*(\omega) = \gamma_j(-\omega)$  (see App. A), we model the low-frequency behavior of the damping rates as  $\gamma_j(\omega) = \gamma_{0j}|\omega|^s$ , where  $s = 0$  corresponds to the ohmic case. Baths with  $-1 < s < 0$ , for which the damping rate vanishes more slowly than in the ohmic case as  $\omega \rightarrow 0$ , are classified as subohmic. Conversely, baths with  $s > 0$ , where the damping rate vanishes more rapidly, are defined as superohmic. Cases with

$s \leq -1$  are pathological and will not be considered here. Remarkably, given the expression of  $\gamma_j(\omega)$ , the behavior of  $\zeta_{\text{NP}}(\omega)$  near the QPT remains unaffected, leaving the critical point unchanged even for non-ohmic baths. This outcome stands in stark contrast to previous results for the driven-dissipative Dicke model, where the critical point is influenced by the dissipation rate [45–47].

#### IV. INPUT-OUTPUT FIELDS AND SPECTRA

An advantage of the presented approach, in addition to the potential for employing it across a diverse range of parameters and the investigation of non-ohmic dissipation, is the possibility to easily obtain reflection and transmission spectra, both ohmic and non-ohmic. In this section we will focus on constructing the theoretical framework needed, while on the following sections we will apply it to ohmic and non-ohmic (both subohmic and superohmic) cases, presenting as examples the reflection spectra.

From the definition of the Langevin forces (see App. A), containing the bath noise operators  $\tilde{\xi}_j$  ( $j = a, b$ ), we can construct input field operators which are defined as  $\tilde{C}_{\text{in},j} = (2\sqrt{c\gamma})^{-1}\tilde{\xi}_j$ . We notice that, given the absence of the RWA, the input fields  $\tilde{C}_{\text{in},j}$  contain both rotating and counter-rotating terms. Therefore, we have  $F_{\text{in},j} = \pm i\sqrt{2c\gamma_j/\hbar\omega_j}\tilde{C}_{\text{in},j}$ , where the  $+$ ( $-$ ) is associated to the annihilation (creation) operators. In the superradiant phase similar equations hold, upon the introduction of  $2/(\lambda + 1)$  in front of  $\tilde{C}_{\text{in},b}$ , which takes into account the condensation effects (see App. B). Analogously, we can construct quantum Langevin equations for the output fields, which read

$$\tilde{\mathbf{F}}_{\text{out}} = i\mathbf{M}(\mathbf{A}, -\mathbf{\Gamma})\mathbf{v}, \quad (19)$$

where the output field operators are defined similarly to the input case, namely  $F_{\text{out},j} = \pm i\sqrt{2c\gamma_j/\hbar\omega_j}\tilde{C}_{\text{out},j}$  in the normal phase, and with a prefactor of  $2/(\lambda + 1)$  in the superradiant phase. The input-output relations [51, 55] are obtained by combining Eqs. (11) and (19), expressed in terms of input (output) fields,  $\tilde{\mathbf{C}}_{\text{in(ou)},j}$ . Therefore, we obtain

$$\tilde{\mathbf{C}}_{\text{out},j} = \sum_k \sqrt{\frac{\omega_j \gamma_k}{\omega_k \gamma_j}} \mathbf{M}(\mathbf{A}, -\mathbf{\Gamma}) \mathbf{M}(\mathbf{A}, \mathbf{\Gamma})^{-1} \Big|_{jk} \tilde{\mathbf{C}}_{\text{in},k} \quad (20)$$

where  $\mathbf{M}(\mathbf{A}, -\mathbf{\Gamma}) \mathbf{M}(\mathbf{A}, \mathbf{\Gamma})^{-1} \Big|_{jk}$  is the  $(j, k)$ -th  $2 \times 2$  block of the matrix  $\mathbf{M}(\mathbf{A}, -\mathbf{\Gamma}) \mathbf{M}(\mathbf{A}, \mathbf{\Gamma})^{-1}$ , for  $j, k = 1, 2$  ( $= a, b$ ), and  $\tilde{\mathbf{C}}_{\text{in(ou)},j} = (\tilde{C}_{\text{in(ou)},j}, -\tilde{C}_{\text{in(ou)},j}^T)^T$ . We can define, as usual, the scattering matrix  $\mathbf{S}(\omega)$ , whose elements are given by

$$S_{jk} = \left. \frac{\langle \tilde{\mathbf{C}}_{\text{out},j} \rangle}{\langle \tilde{\mathbf{C}}_{\text{in},k} \rangle} \right|_{\langle \tilde{\mathbf{C}}_{\text{in},i} \rangle = 0 \text{ for } i \neq k} \quad (21)$$

As pointed out, the main advantage of the presented approach is the absence of any approximation in the

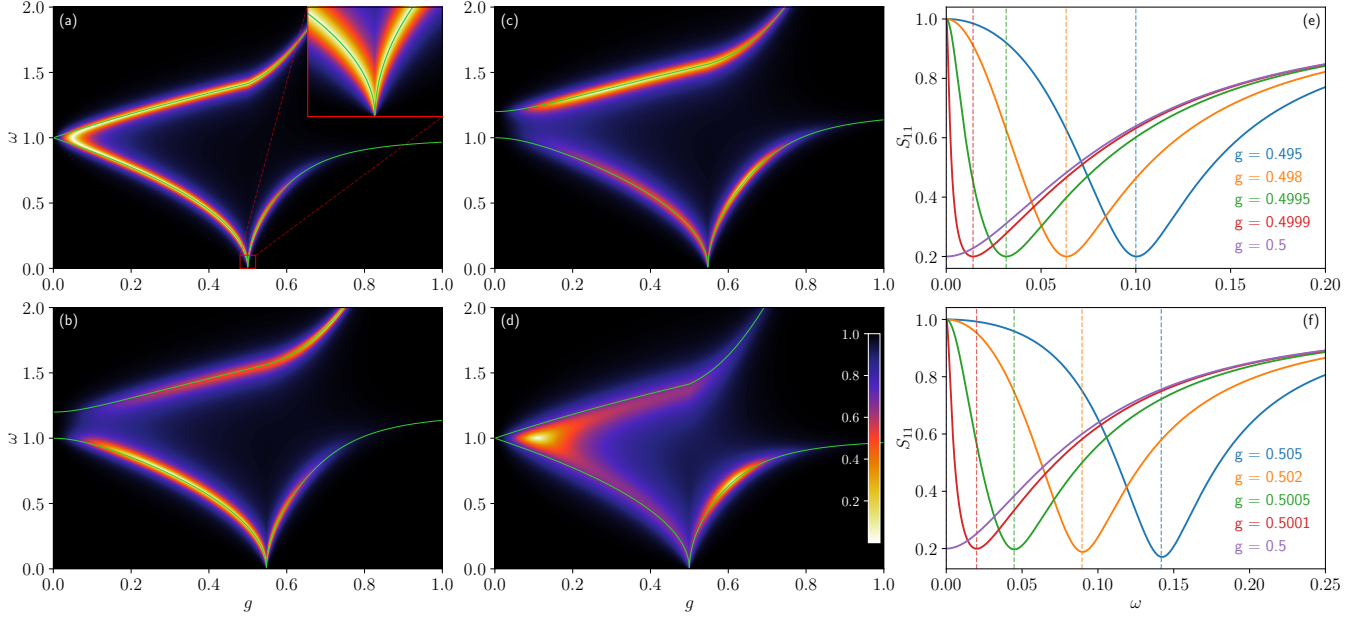


FIG. 4. **Ohmic reflection spectra.** (a-d) 3D reflection spectra in the ohmic case. The corresponding close-system excitation energies are superimposed on the plots. Parameters: (a)  $\omega_a = \omega_b = 1$ ,  $\gamma_a = \gamma_b = 0.1$ ; (b)  $\omega_a = 1.2$ ,  $\omega_b = 1$ ,  $\gamma_a = 0.2$ ,  $\gamma_b = 0.1$ ; (c)  $\omega_a = 1.2$ ,  $\omega_b = 1$ ,  $\gamma_a = 0.1$ ,  $\gamma_b = 0.2$ ; (d)  $\omega_a = \omega_b = 1$ ,  $\gamma_a = 0.1$ ,  $\gamma_b = 0.5$ . (e,f) 2D spectra in the proximity of the critical point. Vertical lines represent the corresponding closed-system excitation energies, showing excellent agreement with the minima of the reflection spectra, both in (e) normal and (f) superradiant phases. Parameters:  $\omega_a = \omega_b = 1$ ,  $\gamma_a = 0.1$ ,  $\gamma_b = 0.15$ .

derivation of Eq. (21), which makes it suitable for describing the system properties in all range of the parameters, even in the most pathological cases. Notably, this includes spectra in the proximity of the critical point or with large losses.

In the following sections we calculate reflection spectra,  $S_{11}$ , through port  $a$  specializing Eq. (20) for  $j = k = 1$ , which yields to

$$\begin{aligned}
 S_{11} &= \frac{\langle \tilde{C}_{\text{out},a} \rangle}{\langle \tilde{C}_{\text{in},a} \rangle} \Big|_{\langle \tilde{C}_{\text{in},b} \rangle = 0} \\
 &= \frac{1}{2} (1, -1) \cdot \mathbf{M}(\mathbf{A}, -\mathbf{\Gamma}) \mathbf{M}(\mathbf{A}, \mathbf{\Gamma})^{-1} \Big|_{11} \cdot \begin{pmatrix} 1 \\ -1 \end{pmatrix} \\
 &= \frac{\zeta(\omega_a, \omega_b, -\gamma_a, \gamma_b)}{\zeta(\omega_a, \omega_b, \gamma_a, \gamma_b)} \quad (22)
 \end{aligned}$$

Eq. (22) is valid for both ohmic and non-ohmic baths. Spectra for alternative input-output channels, such as transmission spectra  $S_{12}$ , can be readily computed by appropriately applying Eq. (21). In the present case, where we consider a single *radiative* input-output port, the system absorption is simply  $\mathcal{A} = 1 - |S_{11}|^2$ .

### A. Ohmic Reflection Spectra

In this section we focus our attention on the study of ohmic spectra ( $s = 0$ ), corresponding to consider damp-

ing rates  $\gamma_j(\omega) = \gamma_{0j}$  in Eq. (22).

In Fig. 4 we plot the reflection spectra for a ohmic bath in a wide range of the parameters, given the absence of approximations in the treatment that could have restricted us. We notice the presence of a Lamb shift in the spectra, which shifts the minima of the reflection with respect to the eigenfrequencies of the isolated system (green solid lines). However, while the Lamb shift is appreciable far away to the critical point, it tends to vanishing in the proximity of  $g_c$ , as highlighted in the inset of panel (a) and panels (e-f). Contextually, the left line broadening of the asymmetric lorentzian goes to zero as fast as the minima, thus consistently describing the spectra even for low frequencies. It must be pointed out that the spectra at *exactly* the critical point is not well-defined for the lower polariton, given its excitation energy being precisely zero. However, this does not represent a problem in real applications and detection, given the fact that it represent a negligible set of zero measure in the coupling domain. We also comment on the differences between panels (b) and (c): while both refer to detuned systems ( $\omega_a = 1.2, \omega_b = 1$ ), in panel (b) the system has an higher damping for the subsystem  $A$  compared to  $B$  ( $\gamma_a = 0.2, \gamma_b = 0.1$ ), whereas viceversa for panel (c). The most noticeable consequence is the depth of the minima in the spectra, different for the upper and lower excitation energies, as we would expect. Lastly, panel (d) presents a more extreme case, for which  $\gamma_b = 0.5$ , thus very off from the Born-Markov approxima-

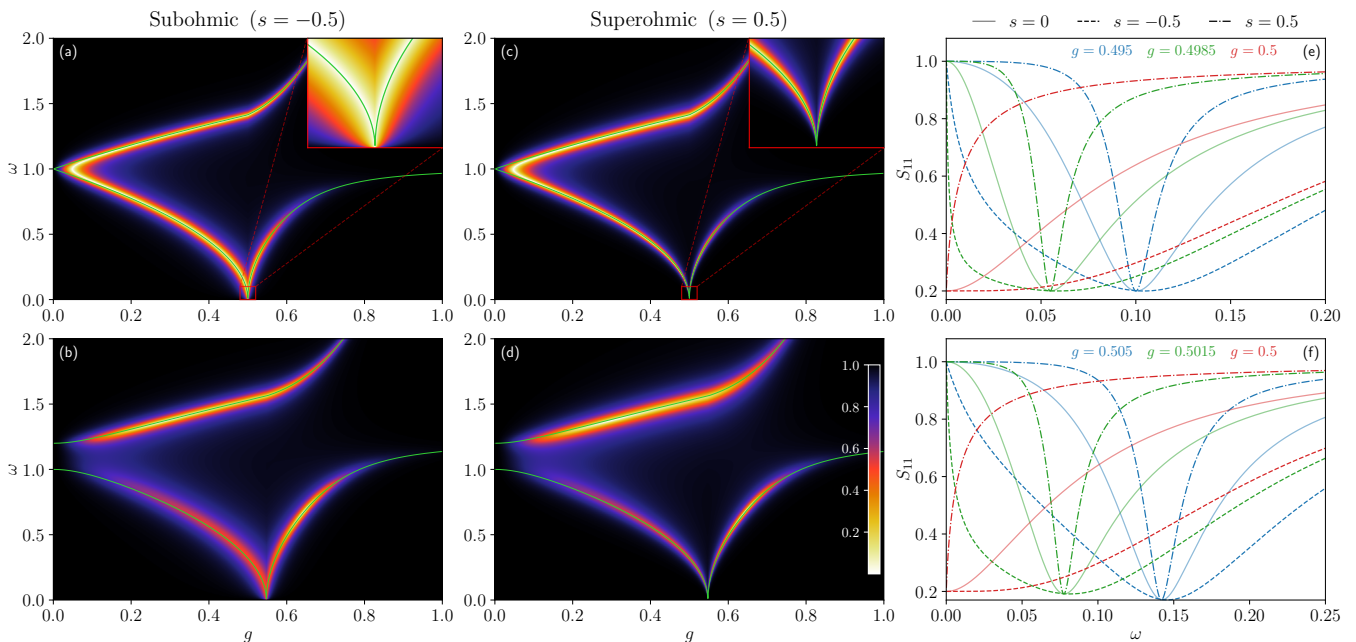


FIG. 5. **Non-ohmic reflection spectra.** (a,b) Reflection spectra in the subohmic case, with the corresponding close-system excitation energies. Parameters: (a)  $\omega_a = \omega_b = 1, \gamma_{0a} = \gamma_{0b} = 0.1$  and (b)  $\omega_a = 1.2, \omega_b = 1, \gamma_{0a} = 0.1, \gamma_{0b} = 0.2$ . (c,d) Reflection spectra in the superohmic case. Parameters: (c)  $\omega_a = \omega_b = 1, \gamma_{0a} = \gamma_{0b} = 0.1$  and (d)  $\omega_a = 1.2, \omega_b = 1, \gamma_{0a} = 0.1, \gamma_{0b} = 0.2$ . The insets highlight the differences, which become evident near the critical point. (e,f) Comparison of the 2D spectra in the proximity of the critical point, both in (e) normal and (f) superradiant phases, for the three different regimes studied: ohmic (solid), subohmic (dashed) and superohmic (dash-dotted). Parameters:  $\omega_a = \omega_b = 1, \gamma_{0a} = 0.1, \gamma_{0b} = 0.15$ .

tion for all couplings. We can notice how considerable is the Lamb shift for low  $g$  and for the upper excitation energy, while still dying out when approaching the critical point in the lower branch, even in this extreme situation. Panels (e,f) present 2D reflection spectra near the critical point (solid lines), along with the corresponding excitation energies of the standard Dicke model described by equation Eq. (2) (dashed lines). These plots illustrate the agreement between the minima of the reflection spectra and the closed-system behavior, confirming the vanishing of the Lamb shift both below (e) and above (f) the critical point.

## B. Non-Ohmic Spectra

In this section, we examine both subohmic and superohmic spectral behaviors. As illustrative examples, we select  $s = -0.5$  for the superohmic case and  $s = 0.5$  for the subohmic case, calculating the reflection spectra using equation Eq. (22). Spectra for other types of baths can be straightforwardly computed using the same procedure.

In Fig. 5(a,b), we present subohmic reflection spectra, utilizing the same parameters as those used in panels (a) and (c) of Fig. 4, respectively. Similarly, Fig. 5(c,d) displays superohmic reflection spectra for the corresponding parameter set. In the subohmic spectra, we observe a

broadening of the full width at half maximum (FWHM) for the lower polariton and a narrowing for the upper polariton compared to the ohmic case. This behavior arises from the frequency-dependent scaling of the damping,  $\gamma_j(\omega) = \gamma_{0j}/\sqrt{\omega}$ , which amplifies losses at low frequencies while reducing them at high frequencies. Conversely, in the superohmic case, characterized by  $\gamma_j(\omega) = \gamma_{0j}\sqrt{\omega}$ , losses are enhanced at high frequencies and suppressed at low frequencies. This behavior is particularly evident in the insets near the critical point shown in Fig. 5(a,c), especially when compared to the inset of Fig. 4(a) for the ohmic bath. Notably, the range of all three insets is identical, highlighting the differences in spectral characteristics. Figure 5(e,f) display a few lower polariton spectra for coupling strength close to the critical point. They show the differences between various baths near the critical point, both below (e) and above (f) the transition. As previously discussed, the behavior precisely at the critical point is pathological; however, it can be safely disregarded as it constitutes a set of zero measure.

## V. CONCLUSIONS

We have presented an exact treatment of the time-independent open Dicke model. The total system-bath Hamiltonian includes the Dicke Hamiltonian in the thermodynamic limit ( $N \rightarrow \infty$ ), the Hamiltonians for sets

of infinite number of harmonic oscillators (the bath normal modes), and the interaction Hamiltonians between the system components and the baths, described by harmonic potentials with metastable minima. This theoretical framework has been applied to describe the open Dicke model in the proximity of the critical point. We have investigated the superradiant phase of the open Dicke model by diagonalizing the full Hamiltonian of the open quantum system. The system dynamics, both in the normal and superradiant phase, has been analyzed by means of proper quantum Langevin equations.

Our results show that the Dicke QPT is resilient to interactions with the environment, at least for a large class of thermal baths with a *well-behaved* density of states (properly vanishing as  $\omega \rightarrow 0$ ). Despite the presence of large Lamb shifts and significant changes of the eigenvalues, we find that the critical point is not affected by the environment, in agreement with recent experimental results [39]. Moreover, in the superradiant phase, the system ground state condensates are not affected by the external environment for system-bath interaction potentials displaying a metastable minimum. On the contrary, we show that the baths get infected by the system and acquire a ground state macroscopic occupation which can be in principle detected. This phenomenon is analogous to the magnetization induced in a material brought into contact with a ferromagnet.

This theoretical framework allowed us to calculate the spectral properties of the system when probed by a coherent weak tone at any value of the critical parameters, for different bath spectral densities and for arbitrary large damping rates. The obtained analytical spectra display lineshapes which become increasingly asymmetric when approaching the critical point.

These results can be readily extended to account for additional dissipation channels, both radiative and non-radiative. Moreover, it is also straightforward to consider nonzero temperature processes. Further investigation is required to ascertain the impact of our approach for driven-dissipative Dicke QPTs. Future studies will extend this framework to nonlinear quantum systems, including the Dicke model with a limited number of emitters. We believe that the rigorous description of the open Dicke model in the proximity of the critical point here presented can also be valuable for criticality-enhanced quantum sensing.

## Appendix A: Quantum Langevin Equations in the Normal Phase

The mutual interaction between a system with a few degrees of freedom and a heat bath with many degrees of freedom represents a fundamental concept in the field of noise physics. The coupling between the bath's numerous variables and the system modifies the system's equations of motion, introducing apparently random terms

that must be accounted for in any analysis. The concept's classic model was first established in Langevin's formulation of the equation that now bears his name. This section aims to derive analogous equations for quantum systems and to apply them to the Dicke model. To this end, we assume that the baths (near their equilibrium, at least) can be described by an infinite set of independent harmonic oscillators. This model becomes exact, e.g., if we are considering electromagnetic baths.

The objective is to derive the quantum Langevin equations for our reference system, which constitutes of two coupled subsystems,  $A$  and  $B$ , that interact with their external environments. The dissipation channels are characterized by the damping rates  $\gamma_a$  and  $\gamma_b$ , respectively. The reference Hamiltonian is given by

$$H = H_{sys} + \frac{1}{2} \sum_{j=a,b} \sum_n [p_{jn}^2 + k_{jn}(q_{jn} - X_j)^2]. \quad (\text{A1})$$

Here,  $H_{sys}$  denotes the system Hamiltonian for the normal ( $H_{NP}$ ) or superradiant ( $H_{SP}$ ) phases, whereas  $X_{a,b}$  represent the coupling operators. This form of coupling is physically meaningful, as it modifies the potential energy based on the deviation of  $X_j$  from each  $q_{jn}$ . In other words, each  $q_{jn}$  is harmonically bounded to the position  $X_j$ , thereby describing fluctuations around this equilibrium position. By applying the following canonical (unitary) transformation

$$\begin{cases} q_n \rightarrow \frac{p_n}{\sqrt{k_n}} \\ p_n \rightarrow -q_n \sqrt{k_n}, \end{cases} \quad (\text{A2})$$

Hamiltonian in Eq. (A1) can be conveniently reformulated as

$$H = H_{sys} + \frac{1}{2} \sum_{j=a,b} \sum_n [(p_{jn} - \sqrt{k_{jn}} X_j)^2 + \omega_{jn}^2 q_{jn}^2]. \quad (\text{A3})$$

By solving the equations of motion for the bath oscillators in terms of the system variables, the *quantum Langevin equations* can be derived [51]:

$$\begin{aligned} \dot{Y}(t) = & \frac{i}{\hbar} [H_{sys}, Y(t)] \\ & - \sum_{j=a,b} \frac{i}{2\hbar} \left[ [X_j, Y], \xi_j(t) - \int_{t_0}^t \dot{X}_j(t') f_j(t-t') dt' \right. \\ & \left. - f_j(t-t_0) X_j(t_0) \right]_+, \end{aligned} \quad (\text{A4})$$

where  $Y$  is an arbitrary system operator,  $[\dots, \dots]_+$  is

the anticommutator and

$$\xi_a(t) = i \sum_n \sqrt{\frac{\hbar k_{an} \omega_{an}}{2}} \left[ c_n^\dagger(t_0) e^{i\omega_{an}(t-t_0)} - c_n(t_0) e^{-i\omega_{an}(t-t_0)} \right]$$

$$\xi_b(t) = i \sum_n \sqrt{\frac{\hbar k_{bn} \omega_{bn}}{2}} \left[ d_n^\dagger(t_0) e^{i\omega_{bn}(t-t_0)} - d_n(t_0) e^{-i\omega_{bn}(t-t_0)} \right]$$

$$f_j(t) = \sum_n k_{jn} \cos(\omega_{jn} t).$$

Here  $\xi_j(t)$  represent the noise terms while  $f_j(t)$  serves as a memory function. The systems  $A$  and  $B$  coupling operators, as already pointed out, are the coordinates  $X_a = a^\dagger + a$  and  $X_b = b^\dagger \sqrt{1 - b^\dagger b/N} + \sqrt{1 - b^\dagger b/N} b$ , respectively. In the normal phase, given the absence of any macroscopic occupation, the system  $B$  coordinate can be approximated in the thermodynamic limit as  $X_b = b^\dagger + b$ . In consideration of the aforementioned definitions, the Langevin equations for our reference system in the normal phase are given by

$$\begin{cases} \dot{a} = -i\omega_a a - ig(b^\dagger + b) \\ \quad - \frac{i}{2\omega_a} \int_{t_0}^t f_a(t-t') [\dot{a}^\dagger(t') + \dot{a}(t')] dt' + \frac{i}{\sqrt{2\hbar\omega_a}} \xi_a \\ \dot{a}^\dagger = i\omega_a a^\dagger + ig(b^\dagger + b) \\ \quad + \frac{i}{2\omega_a} \int_{t_0}^t f_a(t-t') [\dot{a}^\dagger(t') + \dot{a}(t')] dt' - \frac{i}{\sqrt{2\hbar\omega_a}} \xi_a \\ \dot{b} = -i\omega_b b - ig(a^\dagger + a) \\ \quad - \frac{i}{2\omega_b} \int_{t_0}^t f_b(t-t') [\dot{b}^\dagger(t') + \dot{b}(t')] dt' + \frac{i}{\sqrt{2\hbar\omega_b}} \xi_b \\ \dot{b}^\dagger = i\omega_b b^\dagger + ig(a^\dagger + a) \\ \quad + \frac{i}{2\omega_b} \int_{t_0}^t f_b(t-t') [\dot{b}^\dagger(t') + \dot{b}(t')] dt' - \frac{i}{\sqrt{2\hbar\omega_b}} \xi_b \end{cases} \quad (\text{A5})$$

We analyze Eqs. A5 in the frequency domain, assuming that the initial condition is set in the distant past, i.e.,  $t_0 \rightarrow -\infty$ . The aforementioned assumption, combined with the condition that  $f(t)$  is a "well-behaved" function (i.e., highly localized around the zero of its argument), allows the last term in Eq. (A4) to be set to zero. In order to guarantee the causality, we define the decay rate function  $\gamma_j(\omega)$  as the Fourier transform of  $\theta(t)f_j(t)$ , where  $\theta(t)$  is the Heaviside step function, needed in order to preserve causality. In general,  $\gamma_j(\omega)$  can be complex; however, given that  $f_j(t)$  is a real function, it must satisfy the property  $\gamma_j^*(\omega) = \gamma_j(-\omega)$ . In this analysis, we assume that  $\gamma_j$  is real; however, in explicit calculations, there is no restriction against taking it as complex.

Therefore, the resulting quantum Langevin equations for the normal phase in the frequency domain are

$$-i\omega \begin{pmatrix} \tilde{a} \\ \tilde{a}^\dagger \\ \tilde{b} \\ \tilde{b}^\dagger \end{pmatrix} = -i \left( \mathbf{A}_{\text{NP}} - \frac{i}{2} \mathbf{\Gamma}_{\text{NP}} \right) \begin{pmatrix} \tilde{a} \\ \tilde{a}^\dagger \\ \tilde{b} \\ \tilde{b}^\dagger \end{pmatrix} + \tilde{\mathbf{F}}_{\text{in}} \quad (\text{A6})$$

where we defined the Langevin forces vector  $\tilde{\mathbf{F}}_{\text{in}}$  as

$$\tilde{\mathbf{F}}_{\text{in}} = \left( \frac{i}{\sqrt{2\hbar\omega_a}} \tilde{\xi}_a, -\frac{i}{\sqrt{2\hbar\omega_a}} \tilde{\xi}_a, \frac{i}{\sqrt{2\hbar\omega_b}} \tilde{\xi}_b, -\frac{i}{\sqrt{2\hbar\omega_b}} \tilde{\xi}_b \right)^T.$$

Eq. (A6) coincides with Eq. (11) in the main text.

## Appendix B: Quantum Langevin Equations in the Superradiant Phase

To accurately describe the superradiant phase, it is essential to account for the macroscopic coherent occupation of both fields. In order to accommodate this condensation, the bosonic operators have to be shifted as  $a = a_s + \sqrt{\alpha}$  and  $b = b_s - \sqrt{\beta}$ , where  $\alpha$  and  $\beta$  are  $c$ -number of order  $O(\sqrt{N})$ , while  $a_s$  and  $b_s$  are still bosonic operators describing the fluctuations around their respective mean values. Given these relations and the definition of the system coordinates, we obtain the effective system coupling operators  $X_a = a_s^\dagger + a_s + 2\sqrt{\alpha}$  and  $X_b = b_s^\dagger \sqrt{\theta} + \sqrt{\theta} b_s - 2\sqrt{\beta} \sqrt{\theta}$  for systems  $A$  and  $B$ , respectively, where  $\theta = 1 - [b_s^\dagger b_s - \sqrt{\beta}(b_s^\dagger + b_s)](N - \beta)^{-1}$ . In this framework, the condensation in the closed system could induce a corresponding condensation in the thermal baths. Therefore, to accommodate this possibility, the bath operators also have to be shifted as

$$c_m = c_{s,m} + i\sqrt{\tau_m} \rightarrow \begin{cases} p_{am} = i\sqrt{\frac{\omega_{am}}{2}} (c_{s,m}^\dagger - c_{s,m}) + \sqrt{2\omega_{am}\tau_m} \\ q_{am} = \frac{1}{\sqrt{2\omega_{am}}} (c_{s,m}^\dagger + c_{s,m}) \end{cases}$$

The operator  $d_n$  for bath  $B$  is shifted in a similar manner as  $d_n = d_{s,n} - i\sqrt{\sigma_n}$ . Here,  $\tau_m$  and  $\sigma_n$  are  $c$ -numbers of order  $O(N)$  describing the bath mode macroscopic occupations, while  $c_{s,m}$  and  $d_{s,n}$  are bosonic operators that describe the fluctuations around their respective mean values.

Upon substituting the aforementioned definitions into equation Eq. (A1), and considering the thermodynamic limit, we obtain the complete Hamiltonian to be minimized

$$\begin{aligned}
H = & \omega_a a_s^\dagger a_s + \left[ 2g \sqrt{\frac{\alpha\beta}{N(N-\beta)}} + \omega_b \right] b_s^\dagger b_s - \left[ 2g \sqrt{\frac{\beta(N-\beta)}{N}} - \omega_a \sqrt{\alpha} \right] (a_s^\dagger + a_s) \\
& + \left[ 2g(N-2\beta) \sqrt{\frac{\alpha}{N(N-\beta)}} - \omega_b \sqrt{\beta} \right] (b_s^\dagger + b_s) + \frac{g(2N-\beta)}{2(N-\beta)} \sqrt{\frac{\alpha\beta}{N(N-\beta)}} (b_s^\dagger + b_s)^2 \\
& + g(N-2\beta) \sqrt{\frac{1}{N(N-\beta)}} (a_s^\dagger + a_s)(b_s^\dagger + b_s) \\
& + \frac{1}{2} \sum_m \frac{\omega_{am}}{2} (c_{s,m}^\dagger + c_{s,m})^2 \\
& + \frac{1}{2} \sum_m \left\{ \left[ i \sqrt{\frac{\omega_{am}}{2}} (c_{s,m}^\dagger - c_{s,m}) \right]^2 + 2i\omega_{am} \sqrt{\tau_m} (c_{s,m}^\dagger - c_{s,m}) + k_{am} [(a_s^\dagger + a_s)^2 + 4\sqrt{\alpha} (a_s^\dagger + a_s)] \right\} \\
& - \sum_m \sqrt{k_{am}} \left\{ i \sqrt{\frac{\omega_{am}}{2}} (c_{s,m}^\dagger - c_{s,m}) (a_s^\dagger + a_s) + i\sqrt{2\omega_{am}} \sqrt{\alpha} (c_{s,m}^\dagger - c_{s,m}) + \sqrt{2\omega_{am}} \sqrt{\tau_m} (a_s^\dagger + a_s) \right\} \\
& + \frac{1}{2} \sum_n \frac{\omega_{bn}}{2} (d_{s,n}^\dagger + d_{s,n})^2 \\
& + \frac{1}{2} \sum_n \left\{ \left[ i \sqrt{\frac{\omega_{bn}}{2}} (d_{s,n}^\dagger - d_{s,n}) \right]^2 - 2i\omega_{bn} \sqrt{\sigma_n} (d_{s,n}^\dagger - d_{s,n}) \right\} \\
& + \frac{1}{2} \sum_n k_{bn} \left\{ \left( 1 - \frac{4\beta}{N-\beta} \right) (b_s^\dagger + b_s)^2 + 4\sqrt{\beta} \left( \frac{\beta}{N-\beta} - 1 \right) (b_s^\dagger + b_s) - \frac{4\beta}{N-\beta} b_s^\dagger b_s \right\} \\
& - \sum_n \sqrt{k_{bn}} \left\{ i \sqrt{\frac{\omega_{bn}}{2}} \left( 1 - \frac{\beta}{N-\beta} \right) (d_{s,n}^\dagger - d_{s,n}) (b_s^\dagger + b_s) - \sqrt{2\omega_{bn}} \left[ i \sqrt{\beta} (d_{s,n}^\dagger - d_{s,n}) \right. \right. \\
& \quad \left. \left. + \left( 1 - \frac{\beta}{N-\beta} \right) \sqrt{\sigma_n} (b_s^\dagger + b_s) + \frac{\sqrt{\beta} \sqrt{\sigma_n}}{2(N-\beta)} \left( 1 + \frac{\beta}{2(N-\beta)} \right) (b_s^\dagger + b_s)^2 + \frac{\sqrt{\beta} \sqrt{\sigma_n}}{N-\beta} b_s^\dagger b_s \right] \right\} \quad (B1)
\end{aligned}$$

Enforcing an equilibrium condition on Eq. (B1) (which corresponds to setting the linear terms in the bosonic operators to zero), we find that the modes in the superradiant phase exhibit non-zero macroscopic occupations. These are expressed as follows

$$\begin{cases} \alpha = \frac{Ng^2}{\omega_a^2} \left( 1 - \frac{1}{\lambda^2} \right) \\ \beta = \frac{N}{2} \left( 1 - \frac{1}{\lambda} \right) \\ \tau_m = 2 \frac{k_{am}}{\omega_{am}} \alpha \\ \sigma_n = 2 \frac{k_{bn}}{\omega_{bn}} \beta, \end{cases} \quad (B2)$$

where  $\lambda = 4g^2/(\omega_a \omega_b)$ . As can be seen, the values of  $\alpha$  and  $\beta$  that minimize the total Hamiltonian of the open system are identical to those in the closed system in Eq. (5).

Consequently, under these conditions, the effective Hamiltonian for the superradiant phase becomes

$$H = H_{\text{SP}} + \frac{1}{2} \sum_{j=a,b} \sum_n \left[ \left( \rho_{jn} - \sqrt{k_{jn}} x_j \right)^2 + \omega_{jn}^2 q_{jn}^2 \right], \quad (B3)$$

coinciding with Eq. (16) in the main text. It can be observed that the Hamiltonians in equations Eq. (A3) and

Eq. (B3) are formally identical, with the only difference being that the bare operators are replaced by the shifted ones and the coupling is renormalized. Therefore, this latter equation defines the effective coupling operators,  $x_a = a_s^\dagger + a_s$  and  $x_b = b_s^\dagger + b_s$ , and the renormalized couplings,  $\tilde{k}_{an} = k_{an}$  and  $\tilde{k}_{bn} = 4k_{an}/(\lambda+1)^2$ , in the superradiant phase. Hence, the Langevin equations can be expressed as follows

$$\begin{cases} \dot{a}_s = -i\omega_a a_s - i\tilde{g}(b_s^\dagger + b_s) \\ \quad + \frac{1}{2} \int_{-t_0}^t f_a(t-t') (a_s^\dagger(t') - a_s(t')) dt' + \frac{i}{\sqrt{2\hbar\omega_a}} \xi_a \\ \dot{a}_s^\dagger = i\omega_a a_s^\dagger + i\tilde{g}(b_s^\dagger + b_s) \\ \quad - \frac{1}{2} \int_{-t_0}^t f_a(t-t') (a_s^\dagger(t') - a_s(t')) dt' - \frac{i}{\sqrt{2\hbar\omega_a}} \xi_a \\ \dot{b}_s = -i\tilde{\omega}_b b_s - i\tilde{g}(a_s^\dagger + a_s) - 2iD(b_s^\dagger + b_s) \\ \quad + \frac{1}{2} \left( \frac{2}{\lambda+1} \right)^2 \int_{-t_0}^t f_b(t-t') (b_s^\dagger(t') - b_s(t')) dt' + \frac{i}{\sqrt{2\hbar\tilde{\omega}_b}} \frac{2}{\lambda+1} \xi_b \\ \dot{b}_s^\dagger = i\tilde{\omega}_b b_s^\dagger + i\tilde{g}(a_s^\dagger + a_s) + 2iD(b_s^\dagger + b_s) \\ \quad - \frac{1}{2} \left( \frac{2}{\lambda+1} \right)^2 \int_{-t_0}^t f_b(t-t') (b_s^\dagger(t') - b_s(t')) dt' - \frac{i}{\sqrt{2\hbar\tilde{\omega}_b}} \frac{2}{\lambda+1} \xi_b \end{cases} \quad (B4)$$

where  $\tilde{\omega}_b$ ,  $\tilde{g}$  and  $D$  are defined in the main text. The preceding system of equations can be reformulated in a more condensed format within the frequency domain, in

accordance with the procedure delineated in App.A:

$$-i\omega \begin{pmatrix} \tilde{a}_s \\ \tilde{a}_s^\dagger \\ \tilde{b}_s \\ \tilde{b}_s^\dagger \end{pmatrix} = -i \left( \mathbf{A}_{\text{SP}} - \frac{i}{2} \mathbf{\Gamma}_{\text{SP}} \right) \begin{pmatrix} \tilde{a}_s \\ \tilde{a}_s^\dagger \\ \tilde{b}_s \\ \tilde{b}_s^\dagger \end{pmatrix} + \begin{pmatrix} \frac{i}{\sqrt{2\hbar\omega_a}} \tilde{\xi}_a \\ -\frac{i}{\sqrt{2\hbar\omega_a}} \tilde{\xi}_a \\ \frac{i}{\sqrt{2\hbar\omega_b}} \lambda+1 \tilde{\xi}_b \\ -\frac{i}{\sqrt{2\hbar\omega_b}} \lambda+1 \tilde{\xi}_b \end{pmatrix} \quad (\text{B5})$$

as indicated in Eq. (11).

- 
- [1] R. H. Dicke, Coherence in Spontaneous Radiation Processes, *Phys. Rev.* **93**, 99 (1954).
- [2] K. Hepp and E. H. Lieb, On the superradiant phase transition for molecules in a quantized radiation field: the dicke maser model, *Ann. Phys.* **76**, 360 (1973).
- [3] Y. K. Wang and F. T. Hioe, Phase Transition in the Dicke Model of Superradiance, *Phys. Rev. A* **7**, 831 (1973).
- [4] P. Kirton, M. M. Roses, J. Keeling, and E. G. Dalla Torre, Introduction to the Dicke model: From equilibrium to nonequilibrium, and vice versa, *Adv. Quantum Technol.* **2**, 1800043 (2019).
- [5] B. M. Garraway, The Dicke model in quantum optics: Dicke model revisited, *Philos. Trans. Royal Soc. A* **369**, 1137 (2011).
- [6] G. M. Andolina, F. M. D. Pellegrino, V. Giovannetti, A. H. MacDonald, and M. Polini, Cavity quantum electrodynamics of strongly correlated electron systems: A no-go theorem for photon condensation, *Phys. Rev. B* **100**, 121109 (2019).
- [7] J. Román-Roche, F. Luis, and D. Zueco, Photon Condensation and Enhanced Magnetism in Cavity QED, *Phys. Rev. Lett.* **127**, 167201 (2021).
- [8] S. Sachdev, *Quantum phase transitions* 2nd edn (Cambridge Univ. Press, 2011).
- [9] P. Nataf and C. Ciuti, No-go theorem for superradiant quantum phase transitions in cavity QED and counterexample in circuit QED, *Nat. Commun.* **1**, 72 (2010).
- [10] C. Emary and T. Brandes, Chaos and the quantum phase transition in the Dicke model, *Phys. Rev. E* **67**, 066203 (2003).
- [11] C. Emary and T. Brandes, Quantum Chaos Triggered by Precursors of a Quantum Phase Transition: The Dicke Model, *Phys. Rev. Lett.* **90**, 044101 (2003).
- [12] J. M. Knight, Y. Aharonov, and G. T. C. Hsieh, Are super-radiant phase transitions possible?, *Phys. Rev. A* **17**, 1454 (1978).
- [13] D. Lamberto, O. Di Stefano, S. Hughes, F. Nori, and S. Savasta, Quantum Phase Transitions in Many-Dipole Light-Matter Systems, *arXiv preprint arXiv:2405.10711* (2024).
- [14] G. Andolina, F. Pellegrino, A. Mercurio, O. Di Stefano, M. Polini, and S. Savasta, A non-perturbative no-go theorem for photon condensation in approximate models, *Eur. Phys. J. Plus* **137**, 1 (2022).
- [15] K. Rzażewski, K. Wódkiewicz, and W. Żakowicz, Phase Transitions, Two-Level Atoms, and the  $A^2$  Term, *Phys. Rev. Lett.* **35**, 432 (1975).
- [16] F. Dimer, B. Estienne, A. S. Parkins, and H. J. Carmichael, Proposed realization of the dicke-model quantum phase transition in an optical cavity qed system, *Phys. Rev. A* **75**, 013804 (2007).
- [17] K. Baumann, C. Guerlin, F. Brennecke, and T. Esslinger, Dicke quantum phase transition with a superfluid gas in an optical cavity, *Nature* **464**, 1301 (2010).
- [18] D. Nagy, G. Kónya, G. Szirmai, and P. Domokos, Dicke-Model Phase Transition in the Quantum Motion of a Bose-Einstein Condensate in an Optical Cavity, *Phys. Rev. Lett.* **104**, 130401 (2010).
- [19] Z. Zhiqiang, C. H. Lee, R. Kumar, K. Arnold, S. J. Mason, A. Parkins, and M. Barrett, Nonequilibrium phase transition in a spin-1 dicke model, *Optica* **4**, 424 (2017).
- [20] P. Kirton and J. Keeling, Superradiant and lasing states in driven-dissipative Dicke models, *New J. Phys.* **20**, 015009 (2018).
- [21] D. Nagy and P. Domokos, Nonequilibrium Quantum Criticality and Non-Markovian Environment: Critical Exponent of a Quantum Phase Transition, *Phys. Rev. Lett.* **115**, 043601 (2015).
- [22] D. Nagy and P. Domokos, Critical exponent of quantum phase transitions driven by colored noise, *Phys. Rev. A* **94**, 063862 (2016).
- [23] S. Genway, W. Li, C. Ates, B. P. Lanyon, and I. Lesanovsky, Generalized Dicke Nonequilibrium Dynamics in Trapped Ions, *Phys. Rev. Lett.* **112**, 023603 (2014).
- [24] Corps, Ángel L. and Relaño, Armando, Theory of Dynamical Phase Transitions in Quantum Systems with Symmetry-Breaking Eigenstates, *Phys. Rev. Lett.* **130**, 100402 (2023).
- [25] M. Heyl, Scaling and Universality at Dynamical Quantum Phase Transitions, *Phys. Rev. Lett.* **115**, 140602 (2015).
- [26] M. Heyl, Dynamical quantum phase transitions: a review, *Rep. Prog. Phys.* **81**, 054001 (2018).
- [27] A. A. Zvyagin, Dynamical quantum phase transitions (Review Article), *Low Temp. Phys.* **42**, 971 (2016).
- [28] D. De Bernardis, T. Jaako, and P. Rabl, Cavity quantum electrodynamics in the nonperturbative regime, *Phys. Rev. A* **97**, 043820 (2018).
- [29] O. Viehmann, J. von Delft, and F. Marquardt, Superradiant Phase Transitions and the Standard Description of Circuit QED, *Phys. Rev. Lett.* **107**, 113602 (2011).
- [30] N. Lambert, Y. Matsuzaki, K. Kakuyanagi, N. Ishida, S. Saito, and F. Nori, Superradiance with an ensemble of superconducting flux qubits, *Phys. Rev. B* **94**, 224510 (2016).
- [31] M. Bamba, K. Inomata, and Y. Nakamura, Superradiant Phase Transition in a Superconducting Circuit in Thermal Equilibrium, *Phys. Rev. Lett.* **117**, 173601 (2016).
- [32] S. Ashhab, Y. Matsuzaki, K. Kakuyanagi, S. Saito,

- F. Yoshihara, T. Fuse, and K. Semba, Spectrum of the Dicke model in a superconducting qubit-oscillator system, *Phys. Rev. A* **99**, 063822 (2019).
- [33] P. Nataf, T. Champel, G. Blatter, and D. M. Basko, Rashba Cavity QED: A Route Towards the Superradiant Quantum Phase Transition, *Phys. Rev. Lett.* **123**, 207402 (2019).
- [34] G. Andolina, F. Pellegrino, V. Giovannetti, A. MacDonald, and M. Polini, Theory of photon condensation in a spatially varying electromagnetic field, *Phys. Rev. B* **102**, 125137 (2020).
- [35] D. Guerci, P. Simon, and C. Mora, Superradiant phase transition in electronic systems and emergent topological phases, *Phys. Rev. Lett.* **125**, 257604 (2020).
- [36] A. Mercurio, G. M. Andolina, F. M. D. Pellegrino, O. Di Stefano, P. Jarillo-Herrero, C. Felser, F. H. L. Koppens, S. Savasta, and M. Polini, Photon condensation, Van Vleck paramagnetism, and chiral cavities, *Phys. Rev. Res.* **6**, 013303 (2024).
- [37] A. Ghirri, C. Bonizzoni, M. Maksutoglu, A. Mercurio, O. Di Stefano, S. Savasta, and M. Affronte, Ultrastrong magnon-photon coupling achieved by magnetic films in contact with superconducting resonators, *Phys. Rev. Appl.* **20**, 024039 (2023).
- [38] M. Bamba, X. Li, N. Marquez Peraca, and J. Kono, Magnonic superradiant phase transition, *Commun. Phys.* **5**, 3 (2022).
- [39] Kim, Dasom et al., Observation of the magnonic Dicke superradiant phase transition, *arXiv preprint arXiv:2401.01873* (2024).
- [40] N. Lambert, C. Emary, and T. Brandes, Entanglement and the Phase Transition in Single-Mode Superradiance, *Phys. Rev. Lett.* **92**, 073602 (2004).
- [41] Y. Chu, S. Zhang, B. Yu, and J. Cai, Dynamic framework for criticality-enhanced quantum sensing, *Phys. Rev. Lett.* **126**, 010502 (2021).
- [42] T. Ilias, D. Yang, S. F. Huelga, and M. B. Plenio, Criticality-enhanced quantum sensing via continuous measurement, *PRX Quantum* **3**, 010354 (2022).
- [43] A. Frisk Kockum, A. Miranowicz, S. De Liberato, S. Savasta, and F. Nori, Ultrastrong coupling between light and matter, *Nat. Rev. Phys.* **1**, 19 (2019).
- [44] P. Forn-Díaz, L. Lamata, E. Rico, J. Kono, and E. Solano, Ultrastrong coupling regimes of light-matter interaction, *Rev. Mod. Phys.* **91**, 025005 (2019).
- [45] W. Kopylov, C. Emary, and T. Brandes, Counting statistics of the Dicke superradiance phase transition, *Phys. Rev. A* **87**, 043840 (2013).
- [46] F. Brange, N. Lambert, F. Nori, and C. Flindt, Lee-yang theory of the superradiant phase transition in the open Dicke model, *Phys. Rev. Res.* **6**, 033181 (2024).
- [47] E. G. D. Torre, S. Diehl, M. D. Lukin, S. Sachdev, and P. Strack, Keldysh approach for nonequilibrium phase transitions in quantum optics: Beyond the Dicke model in optical cavities, *Phys. Rev. A* **87**, 023831 (2013).
- [48] T. Holstein and H. Primakoff, Field Dependence of the Intrinsic Domain Magnetization of a Ferromagnet, *Phys. Rev.* **58**, 1098 (1940).
- [49] D. V. Kapor, M. J. Škrinjar, and S. D. Stojanović, Relation between spin-coherent states and boson-coherent states in the theory of magnetism, *Phys. Rev. B* **44**, 2227 (1991).
- [50] G. Grosso and G. Pastori Parravicini, *Solid State Physics* (Academic Press, New York, 2000).
- [51] Gardiner, Crispin and Zoller, Peter, *Quantum noise: a handbook of Markovian and non-Markovian quantum stochastic methods with applications to quantum optics* (Springer Science & Business Media, 2004).
- [52] S. Savasta and R. Girlanda, Quantum description of the input and output electromagnetic fields in a polarizable confined system, *Phys. Rev. A* **53**, 2716 (1996).
- [53] E. Cortese and S. De Liberato, Exact solution of polaritonic systems with arbitrary light and matter frequency-dependent losses, *J. Chem. Phys.* **156**, 084106 (2022).
- [54] Leggett, A. J. and Chakravarty, S. and Dorsey, A. T. and Fisher, Matthew P. A. and Garg, Anupam and Zwerger, W., Dynamics of the dissipative two-state system, *Rev. Mod. Phys.* **59**, 1 (1987).
- [55] Walls, D.F. and Milburn, Gerard J., Input-Output Formulation of Optical Cavities, in *Quantum Optics*, edited by Walls, D.F. and Milburn, Gerard J. (Springer Berlin Heidelberg, Berlin, Heidelberg, 2008) pp. 127-141.